The Tensile Properties of Strain-Crystallizing Vulcanizates. II. Stress Relaxation and Hysteresis

M. Van Der Horst, W. J. McGill, C. D. Woolard

Physical and Polymer Chemistry Research Group, Nelson Mandela Metropolitan University, Port Elizabeth 6031, South Africa

Received 29 March 2005; accepted 22 November 2005
DOI 10.1002/app.23887
Published online in Wiley InterScience (www.interscience.wiley.com).

ABSTRACT: Stress relaxation on cessation of extension and hysteresis were examined in conventional and peroxide vulcanizates over a range of crosslink densities at room temperature and at 90°C. The rate of relaxation decreases with an increase in temperature and is attributed to slower nucleation of strain-induced crystallites. The decrease in the volume fraction of extendable material as a result of strain-induced crystallites has only a small effect on the rate at which the slope of the stress–strain curve rises. Crystallites that form on cooling, melt on heating, leaving an unaltered network, but when strain-induced crystallites are melted by heating, they do not reform on cooling. The relaxed network now extends further before failure than a network in which extension was not interrupted by a heating–cooling cycle. This supports proposals in the preceding article that strain-induced crystals increase tensile properties by altering the network deformation pattern and not by the deflection of propagating flaws, whose mechanism would require the heated sample to fail earlier due to its lower crystalline content. Hysteresis increases sharply at strains at which crystallization in the network becomes possible. The hysteresis ratio reaches a plateau value at higher strains. Relaxation affects both the extension and retraction stress–strain curves and it is proposed that hysteresis is determined by differences in the crystallinity during extension and retraction. © 2006 Wiley Periodicals, Inc. J Appl Polym Sci 101: 2423–2430, 2006

Key words: stress relaxation; hysteresis; conventional and peroxide vulcanizates

INTRODUCTION

This article continues the re-evaluation of the role of strain-induced crystallization in determining the tensile behavior of vulcanizates. More specifically, it looks at stress relaxation caused by strain-induced crystallization. Stress relaxation has been investigated experimentally for NR,[1–4] *Cis*-1,4-polyisoprene (IR),[4] *cis*-1,4-polybutadiene (BR),[5,6] and polychloroprene.[7] At lower extensions ($\lambda < 3$) total relaxation has been observed, i.e., the stress fell to zero, while at higher extensions ($\lambda > 3$), total relaxation did not occur.[1,4,5,7] All these experiments were done at temperatures where normal isothermal crystallization was at a maximum, i.e., −26°C for NR. Flory[8] predicted the extent of stress relaxation to be proportional to the amount of strain-induced crystallization and this was shown to be true at higher elongations ($\lambda > 2$).[1] Gent[1] used an equation (based on Flory's predictions) to estimate the equilibrium degree of crystallization in a stress-relaxed rubber network. It was assumed that no crystallization had occurred at the original stress value when extension ceased.

There are fundamental differences in the morphology of crystals formed under strained and unstrained conditions. Spherulitic structures disappear at higher strains and only γ and/or α filaments are present, depending on the degree of strain.[9–13] Lamellae may nucleate in prestrained samples during isothermal crystallization.[12,14] Crystal nuclei formed during extension should act as physical crosslinks and increase in crosslink density of the network. In a previous study,[15] it was proposed that the lower entropy of shortened chains increases the force required for their continued extension, thus promoting deformation of other less stiff chains in the network. Further nucleation and the continuously altering deformation pattern of network chains lead to progressively higher stresses being required for continued extension and the ultimate tensile strength is raised. On cessation of the extension further strain-induced crystallization will result in stress relaxation, and where such crystallization involves the formation of additional nuclei that can act as physical crosslinks, the slope of the stress–strain curve on re-extension will be steeper than at the point of cessation. The crystalline component will reduce the volume fraction of extendable material and this, too, will increase the slope of the stress–strain curve on further extension.

Correspondence to: C. D. Woolard (christopher.woolard@nmmu.ac.za).

Contract grant sponsor: South African National Research Foundation; contract grant number: GUN 2046777.

No cyclic process is 100% efficient and hysteresis represents the energy loss or nonrecoverable work done on extension of a sample. Hysteresis represents a very large fraction of the energy input and is associated with viscoelastic processes in the network.[16–18] Since hysteresis increases with energy to break, it is contended that viscoelastic processes play an important role in strengthening the network and rubbers with high hysteresis have high tear energies.[16,17] Hysteresis is much higher in strain-crystallizing than in noncrystallizing vulcanizates.[19,20] The amount of crystalline material during retraction has been found to be higher than during extension. Crystalline material has been found to be present until $\lambda = 2$, which is lower than the onset point for crystallization of $\lambda = 3.5$.[21–24]

This article examines the effect of temperature on the rate and extent of stress relaxation in peroxide and conventional vulcanizates, and the effect of temperature changes on the stability and nature of the network formed. It also examines the extent to which crystallization during stress relaxation adds to the physical crosslinks in the network, and analyses the relative importance of additional physical crosslinks, compared to the decrease in the volume fraction of extendable material, on the slope of the stress–strain curve. Hysteresis was measured over a range of crosslink densities at two temperatures and is discussed in terms of stress relaxation and strain-induced crystallization.

EXPERIMENTAL

Vulcanizates

Cis-1,4-polyisoprene (IR) (Nipol IR 2200, Dunlop, Durban, South Africa) was cured with 1 phr dicumyl peroxide (DCP) (Fluka, Steinheim, Germany) to yield a vulcanizate with a crosslink density of 4.66×10^{-5} mol/mL. This compound is referred to as IR/DCP. IR was cured with 3 phr 2-bisbenzothiazole-2,2′-disulfide (MBTS) (Orchem, Sasolburg, South Africa) and 6 phr sulfur (S_8) (AECI, Modderfontein, South Africa) to yield a conventional vulcanizate with a crosslink density of 4.54×10^{-5} mol/mL. This compound is referred to as IR/MBTS. IR/DCP also contained 0.5 phr of the antioxidant *N*-isopropyl-*N*′-phenyl-*p*-phenylenediamine (IPPD) (Bayer, Leverkusen, Germany) and IR/MBTS 1 phr IPPD to prevent oxidation at elevated temperatures. The compounding, vulcanization, and crosslink density determination procedures are given in detail in the first article of this series.[15]

Stress–strain measurements

Tensile test were conducted using an Instron 4411 Tensiometer fitted with a 1 kN load cell and extensions were done at an crosshead extension speed of 500 mm/min. High temperature work was conducted using a thermostated water tank as described in the first article of this series.[15] In most of the experiments, ring-shaped samples were used, which were cut using a nonrotating ring cutter. The rings had an outside diameter of 20 mm and an inner diameter of 16 mm. Ring samples were held in place in the grips by free rotating smooth stainless steel pins 3 mm in diameter. If experiments were conducted out of water, the pins were lubricated with a soapy Teepol solution. A nonstandard size dumbbell sample was also used which had a gauge length of 8 mm and neck width of 2 mm. These were held by self-adjusting elastomeric grips. Because an extensometer could not be used, extensions are expressed as the distance (in mm) traveled by the upper grip.

Crystalline content

The density of strained samples was determined by hydrostatic weighing and was used to calculate the volume fraction of crystalline material. To keep the ring samples in a strained state, a U-shaped stainless steel tube holding frame, with slots at various distances to accommodate the pins holding the samples, was used. The holding frame with samples was suspended in water from a Sartorius 2434 ($d = 1 \times 10^{-5}$ g) analytical balance using 0.3 mm nickel–chrome wire. Ten rubber rings (~2 g in total) were used in density experiments. The mass of rubber in air was first determined followed by the mass in water in an unstrained state. The rings were then stretched using the Instron 4411 Tensiometer. First an extension was done to past the maximum extension to allow for stress softening. This allowed for the use of one set of rubber rings for more than one measurement. The extensions were stopped at various strains and the stretched samples transferred to the holding frame without decreasing the extension. The holding frame was transferred to the water bath and hung from the microbalance. After 30 min, five mass readings were taken and the average was used in the density calculation. The time period between stretching and weighing was to allow for equilibration.

Hysteresis measurements

To calculate hysteresis (W_{hys}), the energy recovered by retraction was subtracted from the energy required for extension (W_i). The areas under the extension and retraction curves yielded the required energy densities (W). Experiments were conducted in the water tank when elevated temperatures were required.

RESULTS

Extent and rate of stress relaxation under equilibrium conditions

Stress relaxation experiments were conducted on IR/MBTS and IR/DCP systems at room temperature (RT)

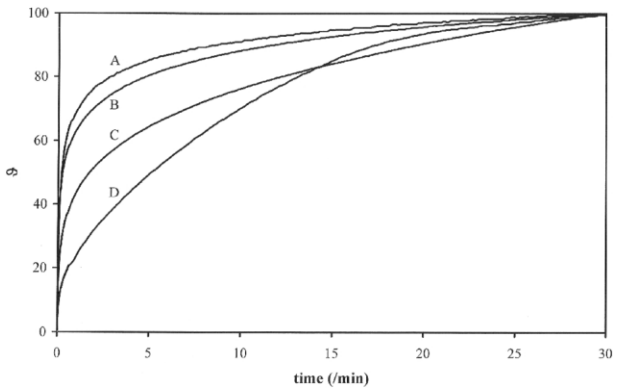

Figure 1 Typical stress relaxation curves (θ) for IR/MBTS extended to various extents of UTS at room temperature and 90°C. (A) 25% of UTS, room temperature; (B) 88% of UTS, room temperature; (C) 75% of UTS, 90°C; (D) 25% of UTS, 90°C.

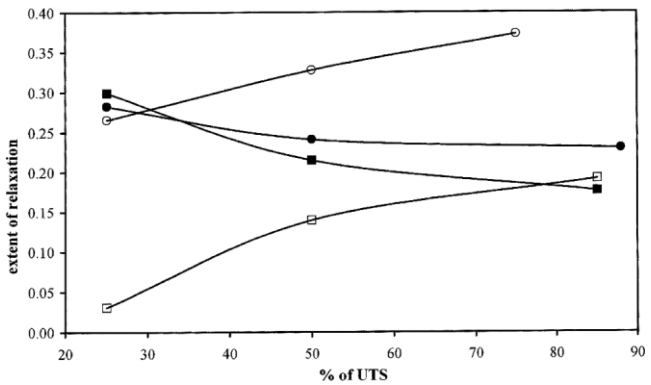

Figure 2 The extent of relaxation of IR/DCP and IR/MBTS at room temperature and 90°C. (○) IR/MBTS, 90°C; (●) IR/MBTS, room temperature; (■) IR/DCP, room temperature; (□) IR/DCP, 90°C.

and at 90°C. Ring samples were employed and were extended to various degrees of their ultimate tensile strength (UTS), usually 25, 50, and 85%. This ensured that stress relaxation both before and after the upturn in the stress–strain curve was measured. The shapes of the relaxation curves were examined by calculating ϑ [eq. (1)], which was plotted against time.

$$\vartheta = \left(\frac{\sigma_i - \sigma_c}{\sigma_i - \sigma_f}\right) \times 100 \quad (1)$$

where σ_i is the initial stress, σ_c is the current stress, and σ_f is the final stress.

The bulk of stress relaxation at RT occurred within the first few minutes. Stress relaxation of IR/DCP was marginally faster than that of IR/MBTS/S_8 as shown in Figure 1. The higher the initial stress, the slower the relaxation. Increasing the temperature to 90°C resulted in a slowing down of relaxation of both vulcanizates. More highly stressed samples initially relaxed more rapidly, but the relaxation curves crossed after 14 min (Fig. 1).

The extent to which the samples relaxed in 30 min is plotted in Figure 2 against the degree of their extension, and is expressed as a percentage of their UTS. Both IR/MBTS and IR/DCP relaxed to a similar extent at RT, the extent of relaxation being the most at the lowest initial stress and the least at the highest initial stress. The situation is very different at 90°C; IR/MBTS relaxed to a larger and IR/DCP to a smaller extent than at RT, while both systems relaxed to larger extents as the initial stress increased.

Crosslink density and volume fraction of extendable material

As discussed previously,[15] strain-induced crystallization leads to an increase in the number of physical crosslinks and load bearing chains, thereby increasing the stress required for extension. To examine the nucleation of further crystalline crosslinks during stress relaxation, the following experiments were conducted. To allow for stress softening, ring samples of both IR/MBTS and IR/DCP systems were extended, at RT, to 85% of their ultimate elongation and returned to zero extension. Each sample was then extended to 75% of its ultimate extension, held for a specific period of time (2, 5, 10, and 30 min) at this extension, and was then extended to 85% of ultimate extension and returned to zero extension. Figures 3 and 4 show that on further extension, the slopes of the stress-extension curves were larger than that of the initial curve at the holding point. In addition, the slopes showed a small, progressive increase with the time held. The increased slopes of the further extensions could be due to the number of crystalline crosslinks increasing and/or the volume of extendable material decreasing as a result of crystal growth.

To investigate the contribution that the decrease in the volume of extendable material makes to the in-

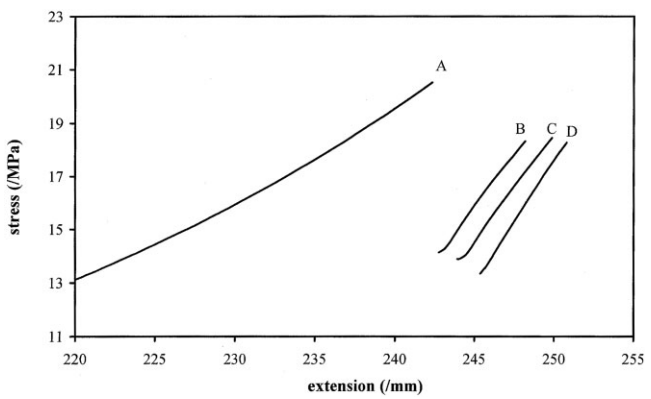

Figure 3 The further extension of IR/MBTS after being held at a an extension for a specific period of time. Only the latter portion of the extension curve is shown. (A) extension, (B) 2 min, (C) 5 min, (D) 10 min.

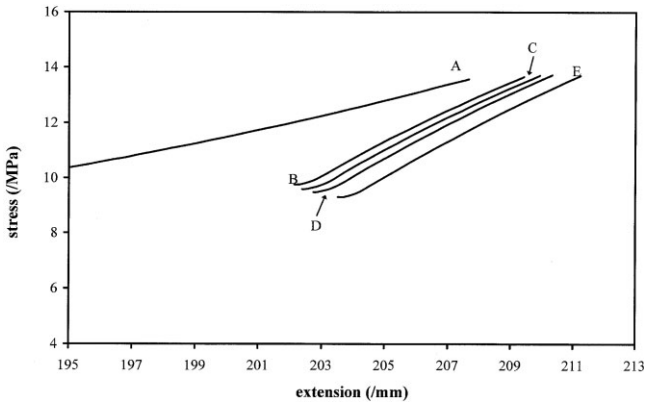

Figure 4 The further extension of IR/DCP after being held at a an extension for a specific period of time. Only the latter portion of the extension curve is shown. (A) extension, (B) 2 min, (C) 5 min, (D) 10 min, (E) 30 min.

crease in the slope of the stress–strain curves seen in Figures 3 and 4, the following experiments were done. A ring sample of IR/MBTS was extended to 200 mm and returned to zero extension to allow for stress softening. It was then extended to 109 mm and held at this extension for 30 min. After being extended for an additional 10 mm, it was returned to zero extension. This procedure was repeated for extensions to 154 and 175 mm (Fig. 5). As in the earlier experiments, the slopes of the curves on further extension were higher than that of the original curve at the point where extension was interrupted, the extent of the increase in slope increasing as the initial extensions increased.

To determine the contribution that the decrease in the volume of extendable material makes, the data was treated in the following manner: The tangent (a) to the extension curve at the point at which the sample was held [origin (Y^0, X^0) (Fig. 6)] was extended to an arbitrary extension value (X^1). Crystallization on stress relaxation should decrease the volume fraction of extendable material, and thus (X^1–X^0) would be decreased by a fraction, equal to the fraction of crystalline material present at X^0 after 30 min, i.e., if crystallization experiments showed that 20% of the material would crystallize at this extension after 30 min, the volume of extendable material and therefore the slope of the stress–strain curve on increasing the stress beyond Y^0 would increase, and a tangent (b) to the re-extension curve at X^0Y^0 would pass through X^2Y^1. A line (c), with a slope equal to the tangent of the experimentally obtained further extension curve was then drawn through the origin (Y^0, X^0) and reached Y^1 at an extension of X^3. If X^3 and X^2 coincided, it would suggest that the increase in slope was entirely due to the decrease in the amount of extendable material, while if $X^3 < X^2$, the decrease in extendable material would only partly have been responsible for the increased slope and further nucleation and the formation of crystalline crosslinks should have accompanied stress relaxation. Table I shows that at all three extensions $X^3 \ll X^2$. It is clear that the major contributor to the increased slope on further extension is the increased number of physical crosslinks, i.e., stress relaxation involves nucleation of a large number of new crystalline crosslinks.

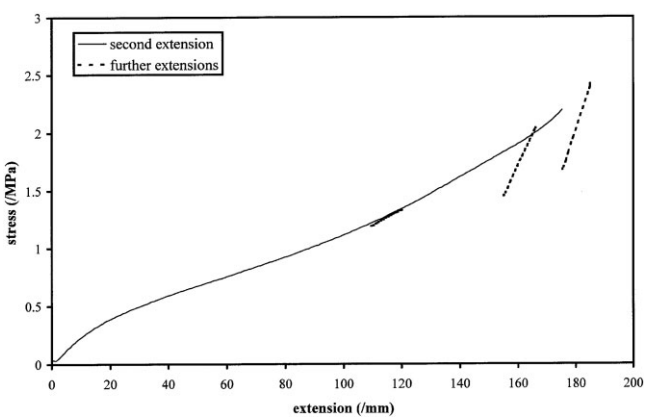

Figure 5 The second and further extensions of IR/MBTS after being held at 109, 154, and 175 mm for 30 min.

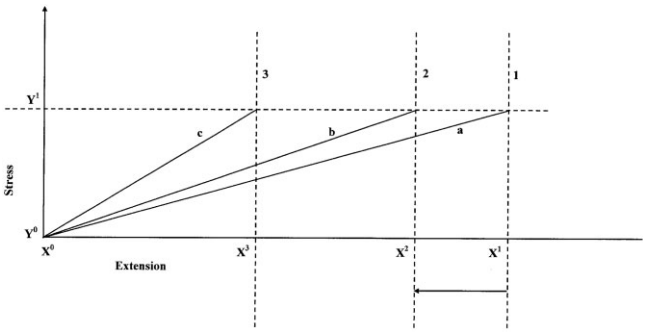

Figure 6 Treatment of data to determine the contribution of volume reduction to further extension.

Stability of strain-induced network

Cooling and reheating

Dumbbell samples of IR/MBTS and IR/DCP were extended at 90°C to two different extensions each (a new sample was used for each extension), held for 30 min, cooled to RT and held at this temperature for 30

TABLE I
The Contribution of the Decrease in Extendable Material to Increased Stress–Strain Slope on Further Extension

Initial extension (X^0) (mm)	X^1–X^0 (mm)	X^2–X^0 (mm)	X^3–X^0 (mm)	% crystallinity
109.5	100.0	95.0	67.0	5
154.6	100.6	84.0	31.0	16
175.0	100.0	78.0	17.2	22

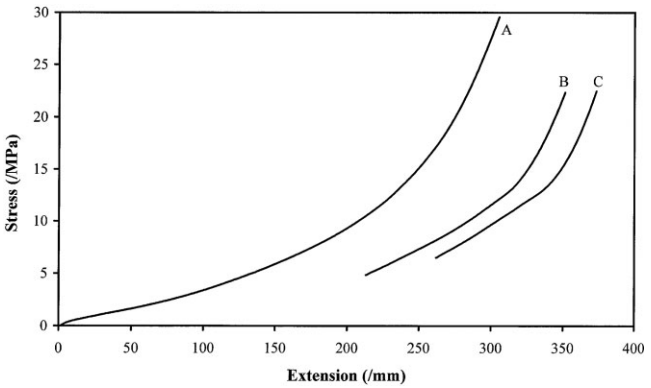

Figure 7 The further extension of IR/MBTS after being held at a extension, heated, and recooled. (A) room temperature extension, (B) and (C) further extensions.

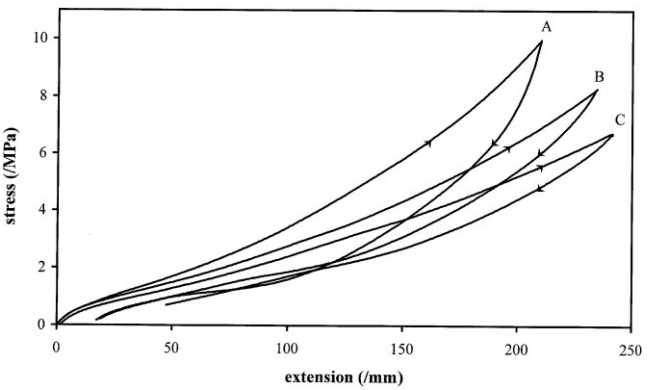

Figure 8 The strain cycles of IR/MBTS/S_8 at different temperatures. (A) 25°C, (B) 60°C, and (C) 90°C.

min, then reheated to 90°C, and held for an additional 30 min. As reported in the literature,[2,4,6] strain-induced crystallization caused the stress to decrease on cooling, while on reheating, the stress returned to its former value. The stress–strain curves of samples that were strained further after heat treatment coincided with those of samples that were not cooled and reheated. Clearly, nucleation and crystal growth on cooling was reversed on reheating.

Heating and recooling

Two ring samples of IR/MBTS were extended at RT to two different extensions and held at these extensions for 30 min. They were then heated to 90°C and kept at this temperature for 30 min, then cooled down to RT and after 30 min, extended till break (Fig. 7). After the heating and cooling process, the samples could extend to a greater extension than possible in an uninterrupted process, though they did break at a slightly reduced stress. The slope of the stress–strain curves at the onset of the further extension was less than in the reference curve at similar strains. The upturn in stress, however, was more abrupt than in the normal extension (Fig. 7).

The crystalline content of ring samples of IR/MBTS, extended at RT to 80% of their ultimate extension and held for 30 min at this extension, was determined by hydrostatic weighing. The samples were then placed in 90°C water for 30 min, cooled back to RT, and the crystalline content determined at various times after cooling (Table II). Clearly heating and recooling had irreversibly changed the stress–strain behavior and the amount of crystalline material present in the strained material.

Effect of temperature on hysteresis

Strain cycles were performed on dumbbell samples of IR/MBTS at three different temperatures to the same input energy density (W_i), with a new sample used for each strain cycle. The strain curves are shown in Figure 8.

Hysteresis was found to decrease with an increase in temperature, in agreement with the observations of Meyer and Ferri.[25] The energy density hysteresis (W_{hys}) and the ratio (β) of W_{hys} and W_i values are shown in Table III.

Effect of crosslink density on hysteresis

With peroxide formulations, the DCP loading was changed to achieve different crosslink densities. With MBTS/S_8 formulations, the MBTS/S_8 ratio was kept constant at 1:2 although the total curative loading was changed. An initial strain cycle was performed to allow for stress softening. Five successive strain cycles, at progressively higher extensions, were then performed on the same sample to the maximum strain of the first strain cycle. The input energy to extend sam-

TABLE II
The Volume Fraction of Crystalline Material in Extended IR/MBTS/S_8 Before Heating, and After Reheating and Cooling

	Crystalline content after heating to 90°C and then cooling (%)			
Initial	30 min	50 min	135 min	210 min
25.3	7.7	8.4	10.4	11.1

TABLE III
The Energy Density Hysteresis (W_{hys}) and β of IR/MBTS/S_8 at Three Different Temperatures

Temperature (°C)	W_{hys} (kJ/m^2)	β
25	0.291	0.338
60	0.195	0.230
90	0.163	0.218

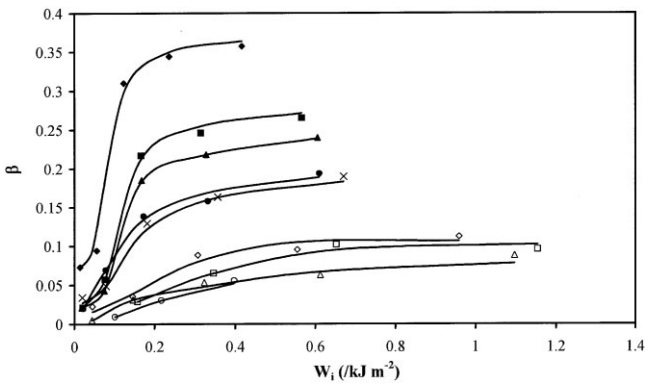

Figure 9 Energy density hysteresis of the IR/MBTS/S_8 vulcanizates at room temperature and 90°C. (♦) 2 phr MBTS/4 phr S_8, room temperature; (■) 3 phr MBTS/6 phr S_8, room temperature; (▲) 4 phr MBTS/8 phr S_8, room temperature; (●) 4.5 phr MBTS/9 phr S_8, room temperature; (×) 5 phr MBTS/10 phr S_8, room temperature; (◊) 2 phr MBTS/4 phr S_8, 90°C; (□) 3 phr MBTS/6 phr S_8, 90°C; (△) 4 phr MBTS/8 phr S_8, 90°C; (○) 4.5 phr MBTS/9 phr S_8, 90°C.

ples to different extensions and β were calculated. These are plotted in Figures 9 and 10. In all samples, β initially had a low value, but then increased sharply as W_i increased before levelling off. The decrease in β for vulcanizates of higher crosslink density indicates a decrease in the extent to which input energy is recoverable at both RT and 90°C. In both systems, the 90°C curves show less of an increase in β with input energy density, and all lie below the lowest RT curve.

DISCUSSION

Rate of relaxation

Stress relaxation that results on cooling of a strained vulcanizate is ascribed to crystallization[1,4–6,8]. Our data show that the isothermal relaxation that occurs on cessation of extension can likewise be ascribed largely to strain-induced crystallization. The decreased rate of stress relaxation at elevated temperatures, compared to RT (Fig. 1), suggests that any viscoelastic processes associated with the time-dependent flow of chains or chain segments within the network, after cessation of extension, do not contribute significantly to stress relaxation. If this were the case, the rate of stress relaxation should increase not decrease with temperature. Instead, the slower relaxation is consistent with a reduced rate of nucleation of crystallites at high temperatures. The formation of a large amount of crystalline material after the cessation of extension, as evidenced by the extent of stress relaxation (Fig. 2) and by an increase in the slope of the stress–strain curve on further extension (Figs. 3 and 4), emphasizes that nonequilibrium conditions apply during extension, and that strain-induced crystallization lags behind the entropy decrease occasioned by extension. The slightly faster relaxation of IR/DCP implies that it crystallizes faster than IR/MBTS. Gent[1] has made a similar observation.

The rate of strain-induced crystallization increases rapidly with an increase in stress[15] and at RT, the slightly slower rate of relaxation at higher extensions (Fig. 1) may be due to a larger portion of strain-induced crystallization having occurred during the extension process, i.e., at the same time interval, after cessation of extension, the relaxation curve reflects a slightly later stage of the overall crystallization process. This is borne out by the lower extent of relaxation at higher extensions in Figure 2. At elevated temperatures, nucleation is slower and this leads to a slower rate of stress relaxation (Fig. 1). Since less crystallization now occurs during the extension phase, the initial rate of relaxation after cessation of extension (Fig. 1) increases with increased stress, though the relaxation curves cross after 14 min. With slower crystallization, more relaxation now occurs after cessation of extension at higher stress values (Fig. 2). Differences in the extent of high temperature relaxation in IR/DCP and IR/MBTS vulcanizates can be ascribed to differences in the network microstructure as will be discussed in the next article in this series.

Crystalline crosslinks and decreased volume fraction of extendable material

Crystallization on cessation of extension is rapid, as indicated by the shape of the stress relaxation curves (Fig. 1). The large change in the slope of the stress–strain curves on re-extension after only 2 min of relaxation (Figs. 3 and 4) shows that crystallization results largely from the formation of new crystallites. At longer relaxation times, nucleation of crystallites continues to contribute to stress relaxation, as can be seen from the higher slopes on re-extension after progres-

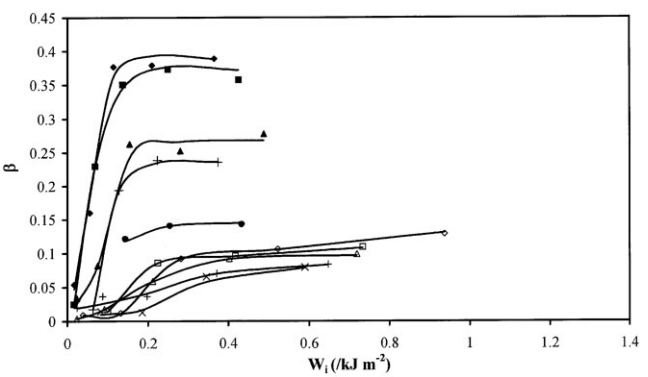

Figure 10 Energy density hysteresis of the IR/DCP vulcanizates at room temperature and 90°C. (♦) 0.4 phr DCP, room temperature; (■) 0.6 phr DCP, room temperature; (▲) 0.8 phr DCP, room temperature; (+) 1 phr DCP, room temperature; (●) 1.6 phr DCP, room temperature; (◊) 0.4 phr DCP, 90°C; (□) 0.6 phr DCP, 90°C; (△) 0.8 phr DCP, 90°C; (○) 1 phr DCP, 90°C; (×) 1.2 phr DCP, 90°C.

sively longer times. Comparison of (X^2–X^0) and (X^3–X^0) in Table I also shows that it is the increased number of strain-induced crosslinks, rather than the decrease in the volume fraction of extendable material, that is the major contributor to the upturn in the stress–strain curves.

Thermal stability and reversibility of networks

As reported in the literature,[2,4,6] on cooling and reheating, samples were found to return to the same stress as applied before cooling. This could indicate that crystals that formed during the cooling phase are smaller, with a higher surface to volume ratio, and therefore less stable on reheating than crystallites already present. If the growth of existing crystals occurred on cooling these would be larger and more stable, resulting in an altered network on reheating. Alternatively, since on cooling crystals form in areas that at 90°C have a high entropy, they would preferentially melt on reheating.

By contrast, in samples subjected to heating and recooling, the smaller slope of the stress–strain curves on further extension (Fig. 7) is indicative of the formation of a network with fewer crosslinks, and this is substantiated by the lower percentage crystallinity (Table II). During the initial extension, the formation of strain-induced crosslinks reduces the length and entropy of chains that form part of the crystallite, and resistance by these shorter, stiffer chains to deformation changes the network deformation pattern.[15] Heating allows the melting of crystalline crosslinks, releases chains from their partially aligned conformations, and allows chains to take up more relaxed conformations, thereby reducing the overall stress and entropy in the network. Consequently, on recooling, there are fewer areas in which the entropy is locally favorable for nucleation. This irreversible process supports earlier proposals[15] that the formation of strain-induced crosslinks during extension alters the deformation pattern of the network, ultimately improving its tensile properties. Changes in the network that allow higher elongation at break of heat-treated samples are akin to changes in the network resulting from delayed crystallization, discussed earlier.[15]

Proposed role of crystallization in hysteresis

Stress relaxation on cessation of extension results from strain-induced crystallization and it is proposed that, in strain-crystallizing vulcanizates, hysteresis is largely associated with strain-induced crystallization. At any extension on the return curve the amount of crystalline material present is larger than that on the extension part of the hysteresis cycle.[21–24] Thus, the stress at a given extension on the return cycle will be lower due to stress relaxation associated with the higher percentage crystallinity at that point, and the return curve drops below that obtained on extension. Toki et al.[22] showed that the extent of hysteresis differed in materials that undergo different amounts of strain-induced crystallization, and they attributed hysteresis to the formation of strain-induced extended-chain crystallites and the transformation of secondary lamella crystals during the retraction cycle. Hysteresis was associated with the extent of crystallization. It is proposed that in strain-crystallizing rubbers hysteresis is related, not to the extent of crystallization in the sample, but to the difference in crystallinity present during the extension and retraction cycles, the difference between the stress at any strain during extension and retraction being due to differences in stress relaxation resulting from the amount of crystallization that has occurred at this point, any variable (temperature, rate of strain) that affects crystallization during extension, will also affect the retraction curve, and hence hysteresis.

Hysteresis curves show a very rapid drop in stress the moment extension is reversed and this can readily be explained in terms of strain-induced crystallization. Toki et al.[22] showed that crystallization continued for a short time interval after reversal of the extension process and, since crystallization at this point is very rapid, stress relaxation and the rate at which the stress–strain curve declines on retraction will be rapid and extensive. This is also implicit in the relaxation that follows on cessation of extension (Fig. 1). Depending on the degree of extension, it takes 30–50 s to complete an extension and return cycle, while crystallization and stress relaxation continue for 30 min and more after cessation of extension, with the largest portion of relaxation occurring during the first minute (Fig. 1). This rapid, initial crystallization gives rise to the stress declining rapidly during a short time interval at the onset of the retraction cycle.

Note that some of the hysteresis will still be due to viscoelastic effects (especially at low extensions) but it is proposed that the bulk of the hysteresis in strain-crystallizing elastomers results from differences in crystallinity between the extension and retraction cycles. This explains why hysteresis is still observed during the 2nd and 3rd extension cycles of a strain-crystallizing elastomer (Fig. 8).

Effect of temperature on hysteresis

Increasing the temperature results in a decrease in hysteresis (Figs. 9 and 10 and Table III). This behavior is well known and is generally attributed to viscoelasticity. It was shown in Figure 1 that the rate of stress relaxation, which relates to crystallization, decreases with an increase in temperature, and it is proposed that the decrease in hysteresis is directly related to slower crystallization, which results in decreased

amounts of crystallization during extension and the early stages of retraction, and not to viscoelastic behavior. Note that as the temperature is raised, the slopes of the stress–strain curves both on extension and retraction become progressively less steep (Fig. 8), consistent with a decrease in rate of crystallization. Slower crystallization means that when retraction occurs, a lower percentage crystallinity will be present, i.e., less stress relaxation has occurred and the stress–strain curve follows a less precipitous path, resulting in less hysteresis. Clearly the area of the hysteresis loop is dependent on the difference between crystallization on extension and retraction.

Effect of crosslink density on hysteresis

The data in Figures 9 and 10 show that at low extensions (low energy input), the hysteresis ratio, β, is very low; most of the energy input being recoverable on retraction. The rapid increase in β coincides with extensions at which strain-induced crystallization becomes possible, while the plateau value indicates that a relatively large, but constant, fraction of input energy is lost at higher extensions. The rate of strain-induced crystallization increases rapidly with strain, and the more rapidly the stress–strain curve rises at higher elongations, the smaller is the difference between the extension and retraction curves at these high extensions. Thus, rapid crystallization at high extensions limits hysteresis losses and accounts for the plots in Figures 9 and 10 reaching plateau values. The plateau also supports the proposal that hysteresis is related to differences in crystallinity on extension and retraction and not simply to the extent of crystallization. At very high extensions, it has been reported[26,27] that the degree of crystallinity achieved on extension reaches a limiting value. The extensions required, however, are in excess of the extensions at which the plateau value of β is observed here.

At RT, β values for peroxide vulcanizates rapidly reach a plateau, while values for conventional vulcanizates continue to rise slowly with energy input (Fig. 9). This is consistent with slower rates of strain-induced crystallization in conventional vulcanizates.

Increased crosslink density impedes crystallization[1,6,23] and the reduced rate of crystallization will decrease hysteresis, as seen in Figures 9 and 10. Increasing temperature similarly decreases the rate of crystallization and β. Crosslink density has a more marked effect on hysteresis at RT than at elevated temperatures, where the rate of crystallization is already reduced. At similar crosslink density, β plateau values are higher for peroxide than for conventional vulcanizates due to the higher rate of crystallization in the former.

CONCLUSIONS

The effect of temperature on the rate and extent of stress relaxation suggests that relaxation is largely associated with strain-induced crystallization, an increase in temperature decreasing the rate of nucleation. On extension, strain-induced crystallization decreases the volume fraction of extendable crystalline material, but this has only a small effect on the rate at which the stress–strain curve rises. The increase in slope is mainly due to chain shortening by strain-induced crystalline crosslinks and the greater stiffness of such shorter chains. Strain-induced crystallites that melt on heating do not reform on cooling, and the now partially relaxed network is able to extend further without fracture than a network that was extended directly to break. This points to the importance of delayed crystallization in relation to network structure and tensile properties. Hysteresis increases rapidly at strains at which strain-induced crystallization becomes possible, but the hysteresis ratio reaches a plateau value at higher extensions, supporting the proposal that hysteresis is largely due to the difference between the degree of crystallinity present on extension and retraction. An increase in crosslink density limits crystallization and reduces hysteresis.

References

1. Gent, A. N. Trans Faraday Soc 1954, 50, 521.
2. Boonstra, B. B. S. T. Ind Eng Chem 1951, 43, 362.
3. Kim, H.; Mandelkern, L. J Polym Sci Part A-2: Polym Phys 1968, 6, 181.
4. Gent, A. N., Kawahara, S.; Zhao, J. Rubber Chem Technol 1998, 71, 668.
5. De Candia, F.; Romano, G. J Appl Polym Sci 1989, 38, 249.
6. Gent, A. N.; Zhang, L. Q. J Polym Sci Part B: Polym Phys 2001, 39, 811.
7. Gent, A. N. J Polym Sci Part A: Gen Pap 1965, 3, 3787.
8. Flory, P. J. J Chem Phys 1947, 15, 397.
9. Andrews, E. H. Proc R Soc London Ser A 1962, 270, 232.
10. Andrews, E. H. Proc R Soc London Ser A 1964, 277, 562.
11. Andrews, E. H. J Polym Sci Part A-2: Polym Phys 1966, 4, 668.
12. Yeh, G. S. Y. Polym Eng Sci 1976, 16, 138.
13. Yau, W.; Stein, R. S. J Polym Sci Part A-2: Polym Phys 1968, 6, 1.
14. Luch, D.; Yeh, G. S. Y. J Appl Phys 1972, 43, 4326.
15. Van der Horst, M.; McGill, W. J.; Woolard, C. D. J Appl Polym Sci, submitted.
16. Smith, T. L. J Polym Sci 1958, 32, 99.
17. Mullins, L. Trans Inst Rubber Ind 1959, 35, 213.
18. Grosch, K.; Harwood, J. A. C.; Payne, A. R. Nature 1966, 212, 497.
19. Harwood, J. A. C.; Payne, A. R. J Appl Polym Sci 1967, 11, 1825.
20. Andrews, E. H.; Fukahori, Y. J Mater Sci 1977, 12, 1307.
21. Mitchell, G. R. Polymer 1984, 25, 1562.
22. Toki, S.; Fujimaki, T.; Okuyama, M. Polymer 2000, 41, 5423.
23. Goppel, J. M.; Arlman, J. J. Appl Sci Res A 1949, 1, 462.
24. Trabelsi, S.; Albouy, P. A.; Rault, J. Rubber Chem Technol 2004, 77, 303.
25. Meyer, K. H.; Ferri, C. Rubber Chem Technol 1935, 8, 319.
26. Tosaka, M.; Kohjiya, S.; Murakami, S.; Poompradub, S.; Ikeda, S.; Sics, I.; Hsiao, B. S. Rubber Chem Technol 2004, 77, 711.
27. Toki, S.; Sics, I.; Hsiao, B. S.; Tosaka, M.; Poompradub, S.; Ikeda, Y.; Kohjiya, S. Macromolecules 2005, 38, 7064.